Activin-A limits Th17 pathogenicity and autoimmune neuroinflammation via CD39 and CD73 ectonucleotidases and Hif1-α–dependent pathways

Ioannis Morianos[a], Aikaterini I. Trochoutsou[a,1], Gina Papadopoulou[a,1], Maria Semitekolou[a], Aggelos Banos[b], Dimitris Konstantopoulos[c], Antigoni Manousopoulou[d], Maria Kapasa[e], Ping Wei[f], Brett Lomenick[g], Elise Belaidi[h,i], Themis Kalamatas[j], Klinta Karageorgiou[k], Triantafyllos Doskas[l], Federica Sallusto[m,n], Fan Pan[f], Spiros D. Garbis[g,2], Francisco J. Quintana[o,p,2], and Georgina Xanthou[a,3]

[a]Cellular Immunology Laboratory, Biomedical Research Foundation of the Academy of Athens, 115 27 Athens, Greece; [b]Division of Immunobiology, Biomedical Research Foundation of the Academy of Athens, 115 27 Athens, Greece; [c]Department of Molecular Biology and Genetics, Biomedical Sciences Research Center "Alexander Fleming", 16672 Athens, Greece; [d]Beckman Research Institute, City of Hope National Medical Center, Duarte, CA 91010; [e]Molecular Biology Laboratory, Biomedical Research Foundation of the Academy of Athens, 115 27 Athens, Greece; [f]Department of Oncology and Medicine, Sidney Kimmel Comprehensive Cancer Center, The Johns Hopkins University School of Medicine, Baltimore, MD 21231; [g]Proteome Exploration Laboratory, Beckman Institute, Division of Biology and Biological Engineering, California Institute of Technology, Pasadena, CA 91125; [h]Laboratoire HP2, University Grenoble Alpes, F-38042 Grenoble, France; [i]INSERM, U1042 Grenoble, France; [j]Department of Neurology, "G. Gennimatas" General State Hospital of Athens, 115 27 Athens, Greece; [k]Department of Neurology, Athens Medical Center, 151 25 Athens, Greece; [l]Department of Neurology, Athens Naval Hospital, 115 21 Athens, Greece; [m]Institute of Microbiology, Eidgenössiche Technische Hochschule, 8093 Zürich, Switzerland; [n]Institute for Research in Biomedicine, Universitá della Svizzera italiana, 6500 Bellinzona, Switzerland; [o]Ann Romney Center for Neurologic Diseases, Brigham and Women's Hospital, Harvard Medical School, Boston, MA 02115; and [p]The Broad Institute of MIT and Harvard, Boston, MA 02115

Edited by Gabriel A. Rabinovich, University of Buenos Aires, Autonomous City of Buenos Aires, Argentina, and approved April 1, 2020 (received for review October 24, 2019)

In multiple sclerosis (MS), Th17 cells are critical drivers of autoimmune central nervous system (CNS) inflammation and demyelination. Th17 cells exhibit functional heterogeneity fostering both pathogenic and nonpathogenic, tissue-protective functions. Still, the factors that control Th17 pathogenicity remain incompletely defined. Here, using experimental autoimmune encephalomyelitis, an established mouse MS model, we report that therapeutic administration of activin-A ameliorates disease severity and alleviates CNS immunopathology and demyelination, associated with decreased activation of Th17 cells. In fact, activin-A signaling through activin-like kinase-4 receptor represses pathogenic transcriptional programs in Th17-polarized cells, while it enhances antiinflammatory gene modules. Whole-genome profiling and in vivo functional studies revealed that activation of the ATP-depleting CD39 and CD73 ectonucleotidases is essential for activin-A–induced suppression of the pathogenic signature and the encephalitogenic functions of Th17 cells. Mechanistically, the aryl hydrocarbon receptor, along with STAT3 and c-Maf, are recruited to promoter elements on *Entpd1* and *Nt5e* (encoding CD39 and CD73, respectively) and other antiinflammatory genes, and control their expression in Th17 cells in response to activin-A. Notably, we show that activin-A negatively regulates the metabolic sensor, hypoxia-inducible factor-1α, and key inflammatory proteins linked to pathogenic Th17 cell states. Of translational relevance, we demonstrate that activin-A is induced in the CNS of individuals with MS and restrains human Th17 cell responses. These findings uncover activin-A as a critical controller of Th17 cell pathogenicity that can be targeted for the suppression of autoimmune CNS inflammation.

cytokines | autoimmune neuroinflammation | Th17 cell differentiation | ectonucleotidases | activin-A

Multiple sclerosis (MS) is a chronic inflammatory demyelinating disease of the central nervous system (CNS) that affects nearly 2.5 million people worldwide (1, 2). The majority of MS patients manifest a relapsing-remitting form (RRMS) that represents the second cause of disability in young adults and is characterized by acute relapses and remissions of neurological deficit (1, 2). Studies in experimental autoimmune encephalomyelitis (EAE), a widely used mouse MS model, have uncovered T helper-type (Th) 17 cells as key drivers of autoimmune neuroinflammation (2, 3). Of clinical relevance, increased frequencies of Th17 cells are detected in the peripheral blood, the cerebrospinal fluid, and the brain of RRMS patients, and in individuals with secondary progressive MS (4–6). Importantly, Th17-related molecules correlate with parameters of MS

Significance

Pathogenic Th17 cells are critical drivers of autoimmune neuroinflammation in multiple sclerosis (MS). We report that administration of the cytokine activin-A ameliorated disease severity in an animal MS model and attenuated CNS neuroinflammation associated with decreased pathogenic Th17 responses. Whole-genome profiling and functional studies revealed that activin-A upregulated the antiinflammatory CD73 and CD39 ectonucleotidases and this was essential for the suppression of the pathogenic signature and encephalitogenic functions of Th17 cells. Mechanistically, activin-A signaling increased antiinflammatory gene expression through activation of the transcription factors AhR, STAT3, and c-Maf and inhibited pathogenic Th17 programs through down-regulation of the metabolic sensor, Hif1-α, and other inflammatory proteins. Of clinical relevance, we show that activin-A restrained pathogenic human Th17 cell responses in MS patients.

Author contributions: I.M., G.P., M.S., F.S., F.P., F.J.Q., and G.X. designed research; I.M., A.I.T., G.P., M.S., A.B., A.M., P.W., and B.L. performed research; E.B. contributed new reagents/analytic tools; T.K., K.K., and T.D. recruited patients and acquired clinical samples; I.M., A.I.T., G.P., M.S., D.K., A.M., M.K., P.W., S.D.G., and G.X. analyzed data; and I.M., S.D.G., F.J.Q., and G.X. wrote the paper.

The authors declare no competing interest.

This article is a PNAS Direct Submission.

Data deposition: The RNA-seq reported in this paper have been deposited in the Gene Expression Omnibus (GEO) database, https://www.ncbi.nlm.nih.gov/geo (accession no. GSE146439). The mass spectrometry proteomics data have been deposited to the ProteomeXchange Consortium via the PRIDE partner repository (dataset identifier PXD017757).

See online for related content such as Commentaries.

[1]A.I.T. and G.P. contributed equally to this work.

[2]S.D.G. and F.J.Q. contributed equally to this work.

[3]To whom correspondence may be addressed. Email: gxanthou@bioacademy.gr.

This article contains supporting information online at https://www.pnas.org/lookup/suppl/doi:10.1073/pnas.1918196117/-/DCSupplemental.

First published May 14, 2020.

activity and relapse frequency (4–6). Hence, the development of therapeutic strategies targeting pathogenic Th17 cell functions is essential for the management of MS.

Accumulating evidence proposes that Th17 cell differentiation and pathogenicity is controlled by specific cytokines and the CNS microenvironment (2–9). For example, Th17 cells differentiated in vitro with IL-6, IL-23, and IL-1β or TGF-β3 exhibit enhanced pathogenic potential and induce autoimmune neuroinflammation upon transfer in vivo (2–10). In contrast, TGF-β1 and IL-6 generate Th17 cells with limited pathogenic activity (2–10). Discrete molecular programs distinguish pathogenic and nonpathogenic Th17 subsets, with high IL-23R, IFN-γ, granulocyte macrophage-colony stimulating factor (GM-CSF), and low CD5L expression characterizing pathogenic cells and increased IL-10, CTLA-4, and c-Maf levels associated with nonpathogenic cells (2–11). Similarly, in humans, Th17 cells coproducing IL-17 and IFN-γ mirror pathogenic Th17 cells, while those expressing IL-17 and IL-10 constitute nonpathogenic cells (12, 13). Elegant studies have corroborated the heterogeneity and plasticity of Th17 cells, demonstrating that Th17 cells, generated in vivo or in vitro under noninflammatory conditions, exhibit increased IL-10 expression and can transdifferentiate into T regulatory (Treg) type 1-like cells (14, 15). Still, the precise factors and molecular pathways that skew pathogenic Th17 cells, generated in the context of highly-inflammatory conditions, such as those occurring during CNS autoimmunity, into nonpathogenic cells remain elusive.

Activin-A is a pleiotropic cytokine that exerts crucial functions in development, hematopoiesis, and stem cell maintenance (16, 17). Activin-A is expressed by the majority of innate and adaptive immune cells and signals through two type I (activin receptor type 1A [or activin receptor-like kinase-ALK2], and activin receptor type 1B [or ALK4]) and two type II (ActRIIA and ActRIIB) receptors (18). Although activin-A and TGF-β belong to the same superfamily, they exert distinct nonredundant, and often opposing, functions associated with their different signaling receptors and the unique repertoire of cell-extrinsic and -intrinsic regulators (17). Activin-A exerts a broad spectrum of pro- and antiinflammatory functions, depending on the type of immune response and the spatiotemporal context (16, 17). Seminal studies have reported instrumental roles of activin-A in the differentiation of mouse Th9 and Foxp3$^+$ Treg cells and follicular Th cells in humans (19–21). Our previous studies have demonstrated that activin-A mitigates Th2 cell-driven allergic responses in experimental asthma and asthmatic individuals, associated with the generation of IL-10–producing Treg cells (22, 23). Still, the effects of activin-A on key aspects of Th17 cell responses, including differentiation and pathogenicity, and the molecular mechanisms involved, remain unexplored.

Here, we report that in vivo administration of activin-A, in a therapeutic regime, attenuates CNS inflammation and demyelination and ameliorates EAE severity. In fact, activin-A signaling through its major type I receptor, ALK4, represses pathogenic transcriptional programs in Th17 cells, while it boosts antiinflammatory gene modules. Whole-genome profiling and functional studies revealed that the ectonucleotidases, CD39 and CD73, are involved in activin-A–induced suppression of Th17 responses. Mechanistic studies demonstrated that activin-A activates the transcription factor (TF), aryl hydrocarbon receptor (AhR), which, along with STAT3 and c-Maf, control CD39 and CD73 expression in Th17 cells. Interestingly, activin-A also negatively regulates inflammatory proteins linked to pathogenic Th17 states, including hypoxia-inducible factor-1α (Hif1-α). Overall, these studies uncover activin-A as a therapeutic target that can be harnessed for the control of Th17 cell-driven autoimmune neuroinflammation.

Results

Activin-A Is Increased in the CNS of Patients with RRMS. Initially, we investigated the expression of activin-A in individuals with RRMS under stable condition (*SI Appendix*, Table S1). Remarkably, our findings demonstrated a marked up-regulation of activin-A levels in the cerebrospinal fluid and the serum of patients with RRMS as compared to controls, pointing to a role of activin-A in the regulation of MS (Fig. 1*A*). Similarly, we detected a substantial increase of activin-A in the spinal cord, serum, and brain of mice undergoing EAE induced by immunization of C57BL/6 mice with myelin oligodendrocyte peptide ($MOG_{35–55}$) peptide emulsified in complete Freund's adjuvant (CFA) (*SI Appendix*, Fig. S1*A*).

In Vivo Administration of Activin-A Attenuates the Clinical Severity of EAE. On the basis of these findings, we investigated the role of activin-A in autoimmune CNS inflammation in vivo. For this, we treated mice with activin-A systemically, every 3 d after EAE onset, in a therapeutic setting. Notably, activin-A administration attenuated EAE severity, as reflected by a significant reduction in the loss of motor function and paralysis throughout the period of clinical evaluation, while control (PBS)-treated mice developed a typical ascending disease (Fig. 1*B*). In support, histopathological analyses revealed markedly reduced immune cell infiltration and demyelination in the spinal cords (Fig. 1*C*). EAE amelioration by activin-A was also associated with significantly decreased frequencies of CNS-infiltrating CD45$^+$CD11b$^+$Ly6C$^+$ inflammatory myeloid cells, as well as IL-17$^+$, IFN-γ$^+$, and IL-17$^+$IFN-γ$^+$ CD4$^+$ T cells (Fig. 1 *D* and *E*). In line with the suppression of inflammatory cell infiltration, activin-A decreased GM-CSF, TNF-α, and IL-1β production in the CNS (Fig. 1*F*). In contrast, IL-10 levels were significantly increased in the spinal cords upon therapeutic activin-A administration (Fig. 1*F*).

To explore the effects of activin-A on encephalitogenic T cell responses, we analyzed the recall response to $MOG_{35–55}$. Flow cytometry analyses revealed that draining lymph node (DLN) cells obtained from activin-A–treated mice at the peak of EAE, contained significantly decreased frequencies of IL-17$^+$, GM-CSF$^+$, IFN-γ$^+$, and IL-17$^+$IFN-γ$^+$ CD4$^+$ T cells upon restimulation ex vivo (Fig. 1*G* and *SI Appendix*, Fig. S1*B*). In contrast, we detected a nearly twofold increase in the percentages of IL-10$^+$ and Foxp3$^+$ CD4$^+$ T cells in mice administered with activin-A, compared to PBS-treated controls (Fig. 1*G* and *SI Appendix*, Fig. S1 *B* and *C*). In agreement with the flow cytometry data, IL-17, GM-CSF, IFN-γ, and TNF-α release in DLN culture supernatants was diminished, concomitant with a marked increase in IL-10 production in mice treated with activin-A (Fig. 1*H*). Collectively, these findings provide evidence that in vivo administration of activin-A ameliorates the clinical severity of EAE associated with decreased encephalitogenic T effector responses.

Activin-A Represses the Pathogenic Signature of Th17 Cells. Based on the suppression of pathogenic Th17-linked effector responses and EAE, we next investigated whether activin-A interferes with Th17 cell differentiation. To investigate this, we polarized naive CD4$^+$ T cells under highly inflammatory Th17-skewing conditions (IL-1β, IL-,6 and IL-23) in the presence of activin-A, and analyzed their global gene-expression profile using RNA sequencing (RNA-seq). Differential expression analysis, summarized in an MA plot and heatmap visualization, uncovered notable differences in the transcriptome of act-A–Th17 cells, with 972 genes significantly regulated (greater than twofold [$\log_2$(FC) < −1 or > 1]), 741 of which were up-regulated and 231 down-regulated, compared to Th17 cells (Fig. 2*A* and *SI Appendix*, Fig. S2*A*). Interestingly, we detected a marked down-regulation of genes related to the pathogenic Th17 signature, such as *Tbx21* and *Batf*, whereas genes associated with nonpathogenic Th17 cells—including *Ahr*, *Maf* and *Ctla4*—were enriched in act-A–Th17 cells (Fig. 2 *A* and *B*) (9–11, 24, 25). Ingenuity pathway analysis (IPA) and gene ontology (GO) studies detected an enrichment of the "role of cytokines in mediating communication between immune cells," "immune cell trafficking," and "inflammatory and cell-mediated immune response" among differentially expressed genes (DEGs) in act-A–Th17 cells (Fig. 2*C*). Moreover, a dense network of molecular interactions associated with AhR signaling, a TF known to affect T cell differentiation (4), was enriched in act-A–Th17 cells (Fig. 2*D*).

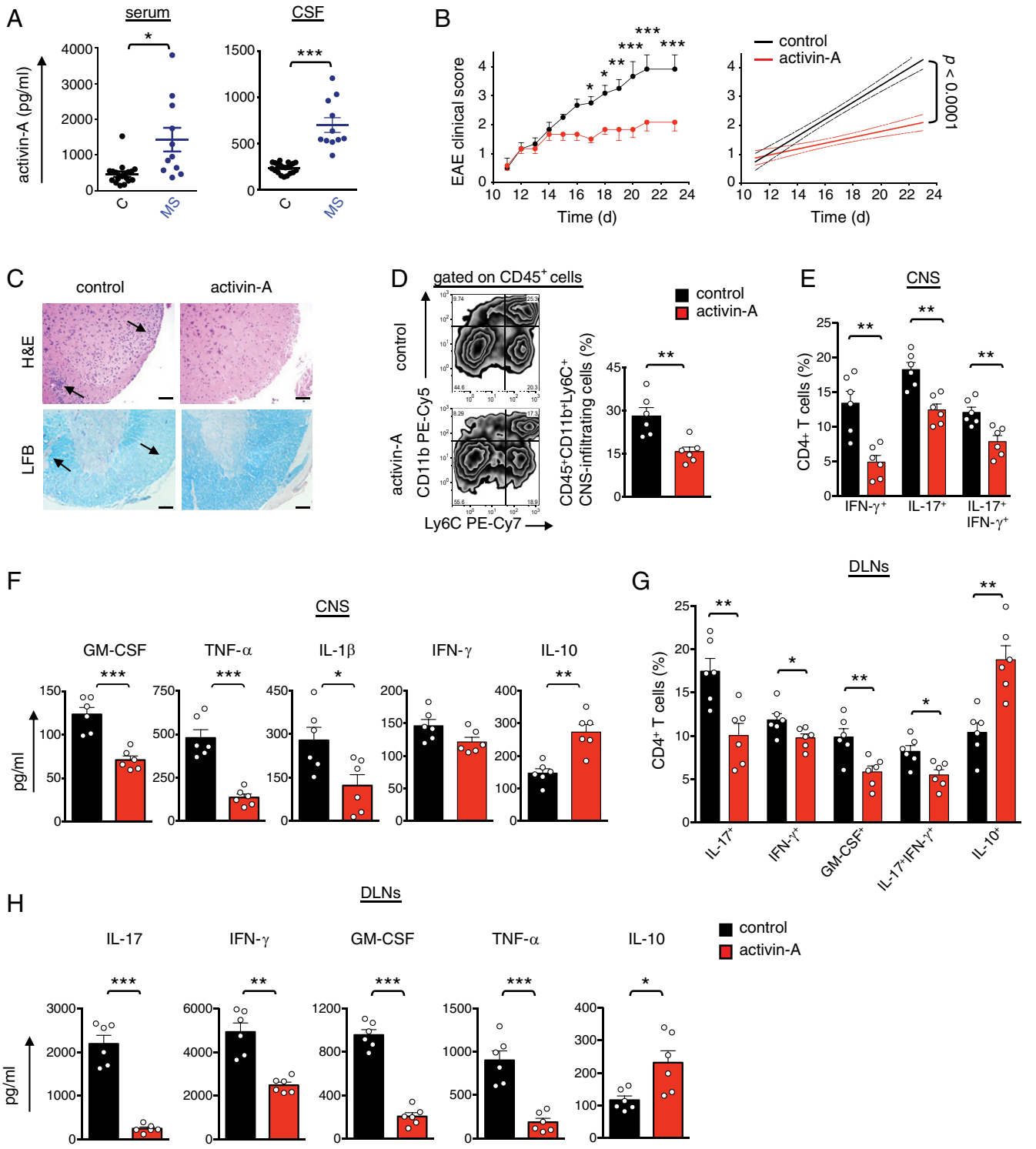

Fig. 1. In vivo administration of activin-A attenuates the clinical severity of EAE. (*A*) Activin-A expression in patients with RRMS ($n = 11$) and disease controls ($n = 20$). Each symbol represents an individual donor. Statistical significance was obtained by the Mann–Whitney *U* test. CSF, cerebrospinal fluid. (*B*) Active EAE was induced in C57BL/6 mice by subcutaneous immunization with $MOG_{35–55}$ peptide in CFA and PTX injection. Activin-A or control (PBS) were administered (intraperitoneally) on disease onset (days 10 to 12) and every 3 d until killed. Clinical scores and regression analysis are depicted. Dashed lines indicate the 95% confidence intervals of the regression lines. Statistical analysis was performed by two-way ANOVA, followed by Bonferroni's multiple comparisons test. (*C*) Representative hematoxylin/eosin (H&E) and Luxol Fast Blue (LFB) stainings on spinal cord sections. (Scale bars, 50 μm.) (*D*) Representative FACS plots (*Left*) and cumulative data (*Right*) showing CNS-infiltrating myeloid cells. (*E*) Cumulative data depicting the percentages of CNS-infiltrating, cytokine-producing $CD4^+$ T cells. (*F*) Cytokine production in spinal cord homogenates. Data are mean ± SEM of triplicate wells and each symbol represents an individual mouse. (*G*) Cumulative data depicting the percentages of cytokine-producing DLN cells in an ex vivo $MOG_{35–55}$ recall assay. (*H*) Cytokine release in DLN culture supernatants. Data are mean ± SEM of triplicate wells. Data in *B–H* are representative of three independent experiments ($n = 6$ mice per group). Statistical significance was obtained by Student's *t* test; $^*P < 0.05$, $^{**}P < 0.01$, and $^{***}P < 0.001$.

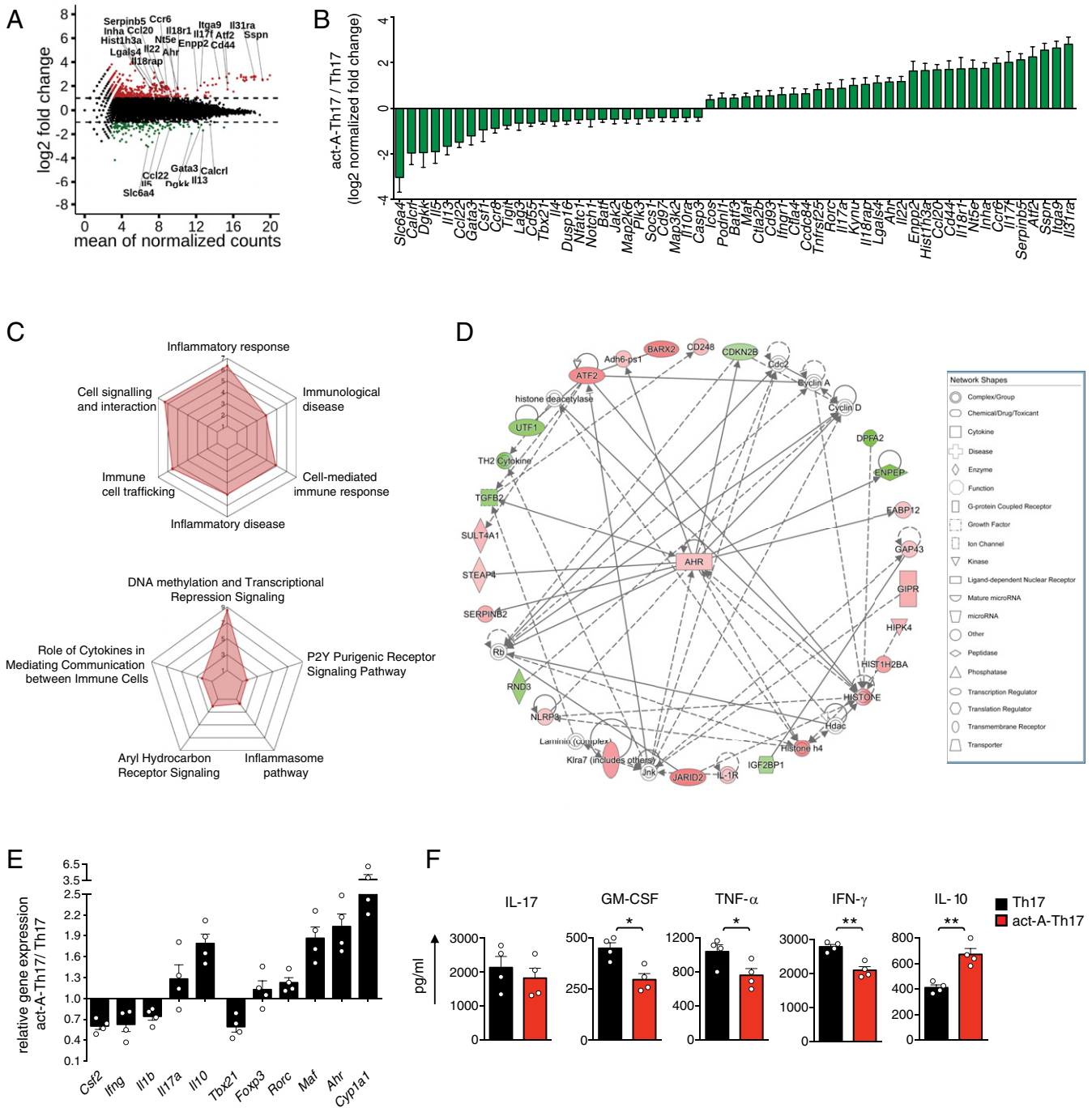

Fig. 2. Activin-A represses the pathogenic signature of Th17 cells. (*A*) Naive CD4$^+$CD62L$^+$ T cells, isolated from the spleens and lymph nodes of C57BL/6 mice, were stimulated with anti-CD3/CD28, IL-1β, IL-6, IL-23, and activin-A (act-A–Th17 cells) or PBS (Th17 cells). Logarithmic fold-changes in gene expression (*y* axis) and the mean of normalized counts (*x* axis) in act-A–Th17 cells versus Th17 cells are presented as an MA plot (red: $\log_2$FC > 1.5, green: *d* FC < −1.5). (*B*) Presentation of 57 DEGs in act-A–Th17 cells relative to Th17 cells. (*C*) Spider plots summarizing a selection of canonical pathways, disease categories, and downstream functions enriched among the 972 DEGs in act-A–Th17 cells. Analyses were performed by IPA and axis values represent the significance level of each finding, expressed in $-\log_{10}$ (*P* value). (*D*) AhR-associated molecular network, as identified among the 972 DEG set, organized in radical layout. Gene-node colors imply up-regulation (red scale), down-regulation (green scale), and no information (white) pertinent to expression changes. Solid edges indicate direct relationships and dashed edges indicate indirect relationships. Data in *A*–*D* are representative of two independent experiments. (*E*) Act-A–Th17 or Th17 cells were generated as in *A*. The gene-expression profile was analyzed by qPCR and normalized to *Gapdh* and *Polr2a*. Each symbol represents the mean ± SEM of duplicate wells and corresponds to one of four independent in vitro experiments. (*F*) Cytokine release in T cell culture supernatants. Each symbol represents the mean ± SEM of triplicate wells and corresponds to one of four independent in vitro experiments. Statistical analysis was performed by unpaired Student's *t* test; $*P < 0.05$ and $**P < 0.01$.

To validate the RNA-seq findings, we carried out qPCR analyses. Indeed, Th17 cells differentiated in the presence of activin-A exhibited decreased expression of *Ifng*, *Csf2*, *Tbx21*, and *Il1b*, genes associated with pathogenic Th17 cell functions, concomitant with enhanced *Il10*, *Ahr*, and *Maf* mRNA levels, linked to nonpathogenic cells (Fig. 2*E*) (9, 13, 26). In support of

the bioinformatics analyses, activin-A up-regulated by nearly fourfold the expression of xenobiotic metabolizing enzyme cytochrome P450 (encoded by *Cyp1a1*), a major AhR transcriptional target (Fig. 2*E*) (21). Cytokine profiling also revealed that activin-A decreased the release of proinflammatory IFN-γ, GM-CSF, and TNF-α in culture supernatants, concomitant with marked increase IL-10 production (Fig. 2*F*). In line with the qPCR data, Foxp3 protein levels remained unaltered in act-A–Th17 cells (*SI Appendix*, Fig. S2*B*). *Il17* and *Rorc* levels were not affected, suggesting that although activin-A decreases expression of critical pathogenic genes, it maintains factors associated with the fundamental Th17 cell program (Fig. 2 *E* and *F*) (8–11, 24, 25). To further validate the suppressive effects of activin-A on the pathogenic Th17 profile, we utilized *Il17a*^{Cre}*R26R*^{eYFP} reporter mice. Briefly, naive CD4$^+$ T cells were sorted from *Il17a*^{Cre}*R26R*^{eYFP} mice, differentiated as above in the presence of activin-A, and their cytokine profile was examined. Consistent with previous reports, we found that cell cultures consisted of eYFP$^+$ Th17 cells expressing IL-17A and eYFP$^-$ Th17 cells, most of which also expressed IL-17A, a finding associated with PMA/ionomycin-mediated induction of intracellular IL-17 before Cre expression leads to deletion of loxp-flanked sequences (*SI Appendix*, Fig. S2*C*) (10, 27). As expected, the frequencies of IL-17$^-$IFN-γ$^+$ and IL-17$^-$IL-10$^+$ CD4$^+$ T cells, along with those of IL-17–secreting γδ$^+$ T cells, were considerably lower to those of Th17 cells, corroborating the differentiation of Th17 cells (*SI Appendix*, Fig. S2 *C* and *D*) (28). Similar to the findings mentioned above, activin-A signaling decreased the percentages of IFN-γ$^+$IL-17$^+$ Th17 cells, considered pathogenic, and increased the frequencies of nonpathogenic IL-10$^+$IL-17$^+$ Th17 cells (*SI Appendix*, Fig. S2*C*).

We next explored whether activin-A represses the differentiation of pathogenic Th17 cells through activation of its canonical signaling pathways. Interestingly, treatment with SIS3, a Smad3 inhibitor, or with an ALK4-blocking antibody, reversed activin-A–driven up-regulation of *Il10*, *Ahr*, and *Maf*, while it restored expression of *Ifng*, *Tnf*, and *Csf2* to levels similar to PBS-treated Th17 cells (*SI Appendix*, Fig. S2*E*). Similarly, GM-CSF, TNF-α, and IFN-γ production was restored in act-A–Th17 cells in the presence of SIS3, whereas activin-A–induced IL-10 increase was abolished (*SI Appendix*, Fig. S2*F*). Altogether, these findings identify activin-A as a negative regulator of pathogenic transcriptional programs in Th17 cells.

Activin-A Restrains the Encephalitogenic Potential of Th17 Cells. In view of the effects of activin-A on the suppression of the pathogenic profile of Th17 cells, we postulated that it may restrain their encephalitogenic functions in vivo. To address this, DLN cells isolated from C57BL/6 mice primed with CFA/MOG$_{35–55}$, were restimulated with MOG$_{35–55}$ in vitro under Th17-polarizing conditions and in the presence of activin-A (9, 10, 27). CD4$^+$ T cells were isolated from DLN cultures and adoptively transferred into *Rag-1*$^{-/-}$ recipients. Remarkably, evaluation of the clinical and histopathological disease progression in *Rag-1*$^{-/-}$ mice reconstituted with act-A–Th17 cells revealed significantly reduced clinical scores and dampened inflammatory cell infiltration and demyelination in the spinal cords as compared to recipients of control-treated Th17 cells (Fig. 3 *A* and *B*). Decreased EAE severity was associated with significantly decreased frequencies of CNS-infiltrating IL-17$^+$, IFN-γ$^+$, GM-CSF$^+$, and IL-17$^+$IFN-γ$^+$ and IL-17$^+$GM-CSF$^+$ CD4$^+$ T cells, whereas the percentages of IL-10$^+$ T cells were increased (Fig. 3*C*). In agreement, GM-CSF, TNF-α, and IL-17 levels in the CNS were decreased, concomitant with a more than twofold increase in IL-10 production (Fig. 3*D*). Consistent with the CNS findings, examination of the recall responses of DLN cells to MOG$_{35–55}$ revealed that T cell proliferation, along with IL-17, GM-CSF, and IFN-γ release, were diminished in recipients of act-A–Th17 cells (*SI Appendix*, Fig. S3*A*). Collectively, these data demonstrate that activin-A restrains the encephalitogenic potential of Th17 cells.

CD73 Signaling Is Essential for Activin-A–Mediated Suppression of Pathogenic Th17 Cell Functions. Interestingly, our whole-genome profiling studies identified *Nt5e* as one of the most up-regulated genes in act-A–Th17 cells (Fig. 2*B*). *Nt5e* encodes the plasma membrane ecto-5′-nucleotidase (CD73) that catalyzes the degradation of adenosine monophosphate (AMP) to adenosine (29, 30). Hence, we next investigated the role of CD73 in the suppressive effects of activin-A on the pathogenic Th17 signature. In line with our RNA-seq data, we found significantly increased CD73 expression in Th17 cells differentiated in the presence of activin-A (Fig. 4 *A* and *B* and *SI Appendix*, Fig. S3*B*). Notably, CD39 (encoded by *Entpd1*) that catalyzes the degradation of extracellular ATP (eATP) into AMP and provides the substrate for CD73 (29, 30), was also up-regulated in act-A–Th17 cells (Fig. 4 *A* and *B* and *SI Appendix*, Fig. S3*B*). Treatment with SIS3 or anti-ALK4 antibody diminished activin-A–triggered increase in *Nt5e* and *Entpd1* expression in Th17 cells (*SI Appendix*, Fig. S3*C*). Interestingly, intracellular cytokine staining showed that CD73$^+$CD39$^+$CD4$^+$ T cells, generated upon

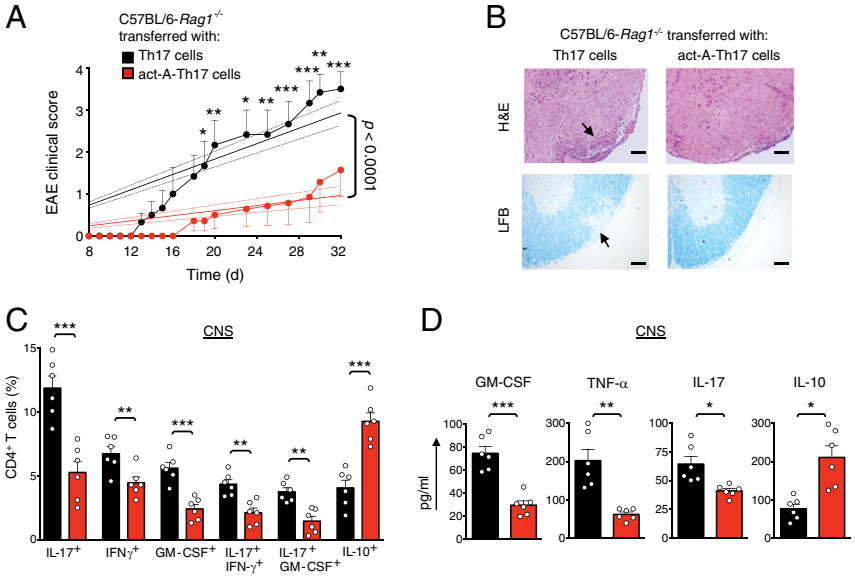

Fig. 3. Activin-A suppresses Th17 cell encephalitogenicity. (*A*) EAE disease scores of C57BL/6-*Rag1*$^{-/-}$ mice reconstituted with CD4$^+$ T cells from CFA/MOG-immunized mice and restimulated for 3 d with MOG$_{35–55}$, IL-23, and activin-A (act-A–Th17 cells) or PBS (Th17 cells). Regression analysis of the clinical scores is also shown. Dashed lines indicate the 95% confidence intervals of the regression lines. Statistical significance was obtained by two-way ANOVA, followed by Bonferroni's multiple comparisons test (n = 6 mice per group). (*B*) Representative hematoxylin/eosin (H&E) staining on spinal cord sections. LFB, Luxol Fast Blue. (Scale bars, 50 μm.) (*C*) Cumulative data showing the percentages of CNS-infiltrating cytokine-producing CD4$^+$ T cells. Each symbol represents an individual mouse. Data are mean ± SEM (n = 6 mice per group). (*D*) Cytokine release in spinal cord homogenates. Data are mean± SEM of triplicate wells (n = 6 mice per group). Statistical significance was obtained by Student's t test; *P < 0.05, **P < 0.01, and ***P < 0.001. Data displayed represent one of two independent experiments.

differentiation of Th17 cells with activin-A, exhibited increased IL-10 production (*SI Appendix*, Fig. S3*D*). Consistent with these in vitro findings, therapeutic administration of activin-A in vivo enhanced CD73 and CD39 expression by $CD4^+$ T cells in the DLNs of mice undergoing EAE (*SI Appendix*, Fig. S3*E*).

Since activin-A up-regulated the expression of CD73, involved in the degradation of eATP to adenosine, we investigated the function of CD73 in act-A–Th17 cells. To address this, we added exogenous ATP and quantified the residual eATP after 8-h incubation. Indeed, we detected reduced concentrations of eATP in culture supernatants of Th17 cells stimulated with activin-A, compared to control-treated Th17 cells (Fig. 4*C*). Conversely, treatment with the CD73 inhibitor, AMP-CP, increased eATP levels, suggesting that CD73 expressed in act-A–Th17 cells promotes eATP catabolism (Fig. 4*C*).

Based on the aforementioned findings, and considering the key role of inflammatory eATP in driving Th17 pathogenicity (29), we interrogated the effects of CD73 on activin-A–mediated modulation of the Th17 profile. Inhibition of CD73 signaling reversed activin-A–induced suppression of *Csf2* and *Ifng* in Th17 cells (Fig. 4*D*). In contrast, AMP-CP decreased activin-A–mediated up-regulation of genes associated with nonpathogenic Th17 cells, such as *Il10*, *Entpd1*, *Ahr*, *Maf*, *Cyp1a1*, and *Nt5e* (Fig. 4*D*). CD73 blockade also reduced activin-A–mediated IL-10 release and restored GM-CSF and IFN-γ production by Th17 cells (Fig. 4*E*).

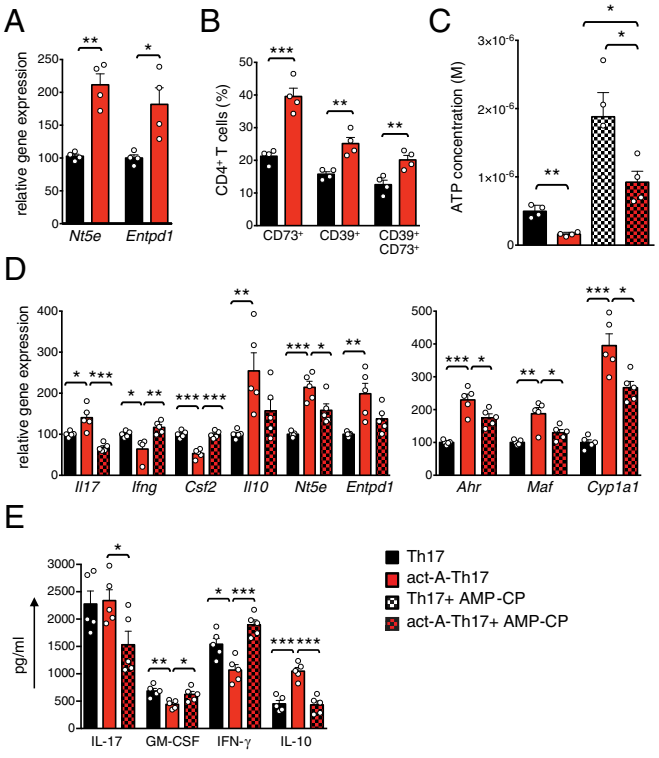

Fig. 4. CD73 signaling is essential for activin-A–mediated repression of the pathogenic Th17 profile. (*A*) The expression of *Nt5e* and *Entpd1* was analyzed by qPCR and normalized to *Gapdh* and *Polr2a*, in act-A–Th17 or Th17 cells. Each symbol represents the mean ± SEM of duplicate wells and corresponds to one of four independent in vitro experiments. (*B*) Cumulative data showing CD39 and CD73 expression, gated on $CD4^+$ T cells. Each symbol represents one of four independent in vitro experiments. (*C*) ATP levels in culture supernatants are shown. Data are mean ± SEM of triplicate wells, each symbol represents one of four independent in vitro experiments. (*D*) Gene expression was analyzed by qPCR and normalized as above. Each symbol is the mean ± SEM of duplicate wells and corresponds to one of five independent experiments. (*E*) Cytokine release in culture supernatants. Each symbol is the mean ± SEM of triplicate wells and corresponds to one of five independent in vitro experiments. Statistical significance was obtained by Student's *t* test; $*P < 0.05$, $**P < 0.01$, and $***P < 0.001$.

To substantiate these in vitro observations, we examined whether in vivo blockade of CD73 signaling reverses activin-A–mediated suppression of Th17 encephalitogenicity. To address this, we isolated DLN cells from CFA/$MOG_{35–55}$-immunized mice and restimulated them in vitro under Th17-polarizing conditions with $MOG_{35–55}$ and activin-A (as described in Fig. 3*A*), in the presence of a CD73 blocking antibody or Ig control. $CD4^+$ T cells were isolated from DLN cultures and transferred into *Rag-1*$^{-/-}$ mice, followed by administration of anti-CD73 or Ig control (experimental protocol in *SI Appendix*, Fig. S4*A*). Recipients of control-treated Th17 cells, administered with anti-CD73 antibody, exhibited heightened EAE scores, compared to mice that received Ig control, consistent with the previously described immunosuppressive effects of CD73 on T cell responses (Fig. 5*A*) (29, 30). Remarkably, in contrast to mice reconstituted with act-A–Th17 cells and administered Ig, mice treated with anti-CD73 displayed earlier EAE onset and exacerbated disease severity (Fig. 5*A*). In addition, histopathological analyses detected increased immune cell infiltration and demyelination in the spinal cords in mice transferred with act-A–Th17 cells upon anti-CD73 administration (*SI Appendix*, Fig. S4*B*). Consistent with the more severe disease phenotype, increased GM-CSF, IFN-γ, and decreased IL-10 levels were observed in the spinal cords (Fig. 5*B*).

To validate and extend the in vivo findings obtained using the anti-CD73 blocking antibody, we performed experiments on *Nt5e*$^{-/-}$ mice. Since previous studies have generated conflicting data, reporting both attenuation and worsening of EAE in *Nt5e*-deficient mice (31–33), we focused our studies on the effects of activin-A on *Nt5e*$^{-/-}$ $CD4^+$ T cells. To this end, we generated MOG-reactive activin-A or control-treated Th17 cells (as above) from CFA/$MOG_{35–55}$-immunized *Nt5e*$^{+/+}$ or *Nt5e*$^{-/-}$ mice and transferred them into *Rag-1*$^{-/-}$ recipients. Indeed, *Nt5e* deficiency in $CD4^+$ T cells interfered with the ability of activin-A to suppress the encephalitogenicity of Th17 cells, resulting in higher EAE scores in recipients of act-A–treated *Nt5e*$^{-/-}$ Th17 cells, as compared to *Rag-1*$^{-/-}$ mice reconstituted with their WT counterparts (*SI Appendix*, Fig. S4*C*). Overall, these findings suggest that CD73 signaling is essential for activin-A–mediated suppression of the pathogenic signature and the encephalitogenic functions of Th17 cells.

AhR Drives CD73 and Antiinflammatory Gene Expression in Th17 Cells in Response to Activin-A. We next investigated the transcriptional mechanisms through which activin-A induces CD73 up-regulation in Th17 cells. Through analyses of published chromatin immunoprecipitation sequencing (ChIP-seq) datasets, we identified enriched ChIP-seq signals for several Th17 cell-associated TFs, including STAT3, c-Maf, and RORγt in the *Nt5e* locus, 1,700 bp downstream the transcription start site (TSS) (*SI Appendix*, Fig. S5*A*) (34–37). We also found a significant enrichment of H3K4me1 and H3K27ac histone modifications surrounding this site, implying an active chromatin state (*SI Appendix*, Fig. S5*A*). In view of these findings, and considering the role of STAT3 in driving CD73 expression in T cells (34), we explored the effects of activin-A on STAT3 activation. Flow cytometry studies revealed that activin-A increased STAT3 phosphorylation in Th17 cells (Fig. 6*A*), while blockade of activin-A canonical signaling pathways decreased STAT3 activation (*SI Appendix*, Fig. S5*B*). Notably, ChIP followed by qPCR analyses demonstrated an enhanced recruitment of STAT3 to its target sequences on the *Nt5e* and on the *Entpd1* promoters in act-A–Th17 cells (Fig. 6*B*) (29, 34). Conversely, inhibition of STAT3 signaling on day 3 following Th17 cell polarization decreased CD39 and CD73 up-regulation in act-A–Th17 cells (Fig. 6 *C* and *E*). STAT3 inhibition also reduced activin-A–mediated up-regulation of IL-10 (Fig. 6*E*). Activin-A did not decrease the mRNA levels of the CD73 transcriptional repressor, growth factor independent-1 (Gfi-1), a mechanism utilized by TGF-β to induce CD73 expression in T cells (*SI Appendix*, Fig. S5*C*) (34).

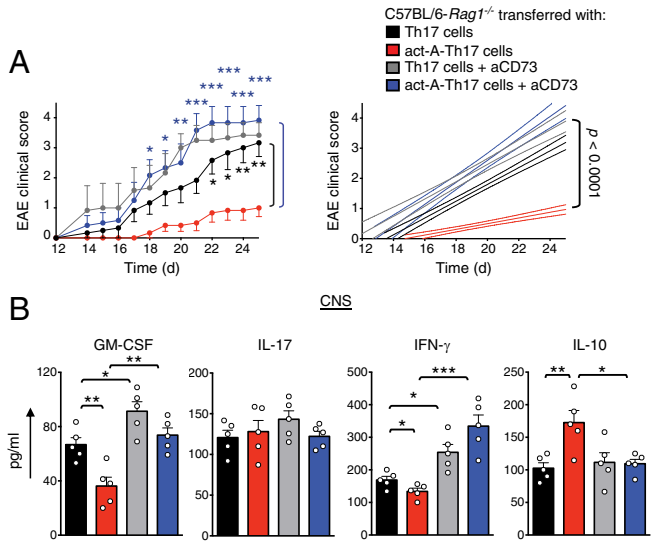

Fig. 5. Blockade of CD73 signaling reverses activin-A–induced suppression of Th17 cell encephalitogenicity. (*A*) EAE disease scores of C57BL/6-*Rag1*$^{-/-}$ mice reconstituted with act-A–Th17 or Th17 cells and treated with anti-CD73 antibody or Ig control (experimental protocol in *SI Appendix*, Fig. S4*A*). Clinical scores (*Left*) and regression analysis (*Right*) are depicted ($n = 5$ mice per group). Statistical significance was obtained by two-way ANOVA, followed by Bonferroni's multiple comparisons test. (*B*) Cytokine levels in spinal cord homogenates. Data are mean ± SEM of triplicate wells; each symbol represents an individual mouse ($n = 5$ mice per group). Statistical analysis was performed by unpaired Student's *t* test; $*P < 0.05$, $**P < 0.01$, and $***P < 0.001$. Data represent one of two independent experiments.

Given that STAT3 inhibition did not completely abolish activin-A–induced *Nt5e* up-regulation in Th17 cells, we explored the roles of AhR and c-Maf, TFs shown to be up-regulated in act-A–Th17 cells (Fig. 2*E*). Indeed, we found increased c-Maf and AhR protein levels in Th17 cells differentiated in the presence of activin-A (Fig. 7 *A* and *B*). Moreover, confocal microscopy studies detected enhanced AhR and c-Maf translocation into the nucleus of act-A–Th17 cells (*SI Appendix*, Fig. S5*D*). Bioinformatics analyses revealed two novel binding sites of AhR and two of c-Maf on the *Nt5e* locus, including the +1,700-bp site (*SI Appendix*, Fig. S5*E*, site 2). Using these genomic segments, we undertook ChIP assays and observed enriched binding of AhR and c-Maf to the +1,700-bp site and also to the −3,600-bp site on the *Nt5e* promoter in act-A–Th17 cells (Fig. 7*C*).

Further bioinformatics analyses of the *Entpd1* promoter identified two previously described AhR binding sites, one of which was in close proximity to a novel c-Maf binding site (*SI Appendix*, Fig. S5*E*). We detected increased binding of AhR on site 1 and site 2 on the *Entpd1* promoter in act-A–Th17 cells, while no differences were observed in c-Maf binding compared to PBS-treated Th17 cells (Fig. 7*D*). Additional data revealed a marked enrichment of AhR binding to its respective site in the *Il10* promoter (−300 bp), along with c-Maf recruitment to its MARE-2 site in act-A–Th17 cells (Fig. 7*E*) (29, 38, 39). As expected, AhR bound to its respective site on the *Cyp1a1* promoter in act-A–Th17 cells (*SI Appendix*, Fig. S5*F*) (26).

Notably, through bioinformatics analyses, we identified a region located in the *Il10* conserved noncoding sequence-9 locus, 9 kb upstream the TSS, wherein STAT3 and AhR were predicted to bind in close proximity. Indeed, through sequential ChIP assays we detected a significant enrichment of both AhR and STAT3 on the *Il10* conserved noncoding sequence-9 locus, previously shown to control *Il10* expression (28), in act-A–Th17 cells (Fig. 7*F*). To further validate these findings, we performed in silico analysis of putative AhR and STAT3 protein–protein interactions. Using the crystal structure of the heterodimeric Hif1-α–ARNT complex with hormone response element DNA as positive control, we proceeded into molecular docking experiments. Interestingly, the docked structure of the known complex of Hif1-α–ARNT showed similar binding affinity (ΔG) and dissociation constant (K_d) values (ΔG = −11.6 Kj/mol, K_d = 3.0e-09) with the docked structure of the AhR-ARNT heterodimer in complex with the dioxin response element and the unphosphorylated mouse STAT3 core fragment (ΔG = −11.3 Kj/mol, K_d = 4.9e-09). Furthermore, superimpositions of the solved structures comprising the docked pose of STAT3-AhR-ARNT showed extremely low RMSD values between the carbon a-atoms (RMSD < 0.01) (*SI Appendix*, Fig. S5*G*). Notably, the docked structure of STAT3-AhR-ARNT remained constant throughout the 10-ns molecular dynamics simulation, and when superimposed with the docking structure before the dynamics simulation, the RMSD value between the carbon a-atoms was calculated to be 0.2 Å. These findings suggest that the proposed docking result of STAT3-AhR-ARNT is highly reliable and exhibits high thermodynamic stability and propose that AhR, ARNT, and STAT3 form a tripartite molecular complex that controls *Il10* in Th17 cells in response to activin-A.

In view of the aforementioned findings showing the effects of AhR on controlling *Nt5e* and *Entpd1* expression in act-A–Th17 cells, we hypothesized that inhibition of AhR signaling would reverse activin-A effects on antiinflammatory gene induction. Indeed, pharmacological inhibition of AhR reversed activin-A–driven *Nt5e*, *Il10*, *Entpd1*, and *Maf* up-regulation in Th17 cells (Fig. 7*G*). In contrast, treatment with CH-223191 restored *Csf2* and *Ifng* levels in act-A–Th17 cells (Fig. 7*G*). As expected, blockade of AhR signaling abrogated activin-A–induced AhR activation, as evidenced by abolished *Cyp1a1* expression (Fig. 7*G*). Similar findings were obtained when IL-10, IFN-γ, and GM-CSF were quantified in culture supernatants (*SI Appendix*, Fig. S5*H*); AhR blockade also suppressed activin-A–induced increase in the frequencies of $CD73^+CD39^+CD4^+$ T cells (*SI Appendix*, Fig. S5*I*). Collectively, these data suggest that AhR directly controls activin-A–induced up-regulation of *Nt5e*, *Entpd1*, and key antiinflammatory genes in Th17 cells.

Hif1-α Suppression Is Crucial for Activin-A–Mediated Modulation of the Pathogenic Th17 Cell Signature. Hif1-α signaling plays a pivotal role in the differentiation of pathogenic Th17 cells (29, 40, 41). Given that activin-A represses transcriptional programs associated with Th17 pathogenicity, we hypothesized that activin-A may negatively regulate Hif1-α responses. Interestingly, Th17 cells differentiated in the presence of activin-A exhibited decreased Hif1-α protein levels (Fig. 8*A*). In support, confocal microscopy studies revealed that whereas Hif1-α was localized mainly in the nucleus of Th17 cells, it mostly accumulated in the cytoplasm of act-A–Th17 cells (*SI Appendix*, Fig. S6*A*). Activin-A signaling did not affect *Hif1α* gene-expression levels, suggesting that it acts via a post-transcriptional mechanism (*SI Appendix*, Fig. S6*B*).

To assess the functional relevance of the suppression of Hif1-α expression for the modulation of the pathogenic Th17 cell signature by activin-A, we conducted Hif1-α overexpression experiments. For this, we crossed LSL-Hif1dPA mice, which conditionally express a form of hemagglutinin-tagged human *HIF1A* cDNA, that escapes recognition by the von Hippel–Lindau tumor-suppressor protein by virtue of proline to alanine substitutions, with a Cd4-Cre mouse strain [Tg(CD4-Cre)1Cwi] (41). In the resulting progeny (hereafter referred to as Hif-Tg/CD4), excision of a floxed stop cassette enables the overexpression of Hif1-α in $CD4^+$ T cells. Indeed, we found that $CD4^+$ T cells isolated from Hif-Tg/CD4 mice and differentiated under Th17-polarizing conditions, in the presence of activin-A, exhibited enhanced expression of signature genes associated with Th17 pathogenicity (Fig. 8*B*). Conversely, overexpression of Hif1-α abrogated activin-A–induced up-regulation of antiinflammatory genes in Th17 cells (Fig. 8*B*).

Subsequently, we explored the molecular mechanisms through which activin-A regulates Hif1-α expression in Th17 cells. In support of the aforementioned qPCR findings, the expression of the Hif1-α inhibitor (encoded by *Hif1an*), known to control

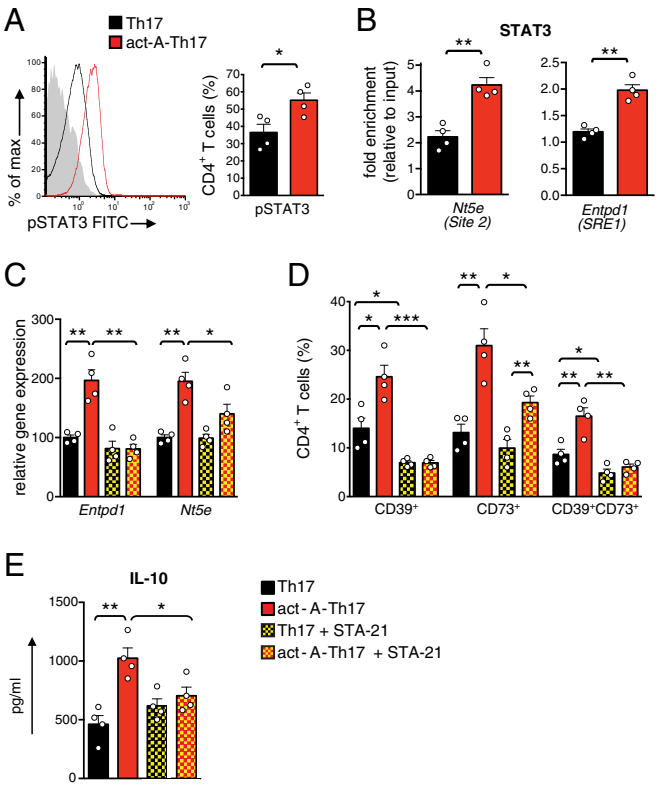

Fig. 6. Activin-A–induced STAT3 activation enhances CD73 expression in Th17 cells. (*A*) Representative FACS plots of Act-A–Th17 or Th17 cells showing pSTAT3 expression. Shaded histogram represents isotype control. Cumulative data are shown as mean ± SEM; each symbol corresponds to one of four independent in vitro experiments. (*B*) ChIP analyses demonstrating the binding of STAT3 on the *Nt5e* locus (site 2, +1,700 bp, *Left*) and on the *Entpd1* promoter, at the SRE1 locus (−3,740 bp) (*Right*). Results are mean ± SEM; each symbol represents the mean ± SEM of duplicate wells and corresponds to one of four independent experiments. (*C*) Act-A–Th17 cells or Th17 cells were cultured in the presence of STA-21. Gene expression was analyzed by qPCR and normalized to *Gapdh* and *Polr2a*. Each symbol represents the mean ± SEM of duplicate wells and corresponds to one of four independent experiments. (*D*) Cumulative data showing the percentages of $CD39^+$, $CD73^+$, and $CD39^+CD73^+$ among $CD4^+$ T cells. Data are mean ± SEM; each symbol corresponds to one of four independent in vitro experiments. (*E*) IL-10 in culture supernatants. Each symbol represents the mean ± SEM of triplicate wells and corresponds to one of four independent experiments. Statistical analysis was performed by unpaired Student's *t* test; $*P < 0.05$, $**P < 0.01$ and $***P < 0.001$.

Hif1-α transcriptionally (42), was not altered in act-A–Th17 cells (*SI Appendix*, Fig. S6*B*). Cycloheximide chase assays demonstrated that, even in the context of disrupted protein translation, HIF1-α levels remained higher in control-treated Th17 cells as compared to act-A–Th17 cells (*SI Appendix*, Fig. S6*C*), suggesting that activin-A signaling affects Hif1-α stability in Th17 cells. Previous studies by our groups have demonstrated that AhR mitigates Hif1-α stability in Tr1 and $Foxp3^+$ Treg cells through binding to the promoters of *Egln1*, *Egln2*, and *Egln3* genes (encoding prolyl hydroxylase domain proteins [Phd]2, Phd1, and Phd3, respectively) and activating Phd-induced Hif1-α degradation (29). In view of the aforementioned findings, we speculated that activin-A may affect Hif1-α stability through *Egln1*, *Egln2*, or *Egln3* induction. Indeed, we detected significantly increased *Egln1* and *Egln2* expression in Th17 cells differentiated in the presence of activin-A (Fig. 8*C*). Moreover, ChIP assays revealed a significant enrichment of AhR binding to its XRE site in the *Egln2* promoter in act-A–Th17 cells (Fig. 8*D*), while inhibition of AhR signaling abrogated activin-A–induced increase in *Egln2* levels (Fig. 8*C*). Altogether, these data suggest that AhR activation triggered by activin-A suppresses pathogenic programs in Th17 cells partly through Phd1-mediated Hif1-α regulation.

To determine whether Phd1 induction was essential for activin-A–mediated modulation of the Th17 signature, we isolated naive $CD4^+$ T cells from *Egln2*$^{-/-}$ mice and differentiated them toward the Th17 lineage, in the presence or absence of activin-A. Notably, *Egln2* deficiency reversed activin-A–induced *Il10*, *Cyp1a1*, *Nt5e*, and *Entpd1* up-regulation, while it restored *Csf2* and *Ifng* levels in Th17 cells (*SI Appendix*, Fig. S6*D*). Still, *Il17*, *Ahr*, and *Maf* expression was not affected by *Egln2* deficiency, suggesting that other members of the Phd family contribute to activin-A effects (*SI Appendix*, Fig. S6*D*).

Activin-A Signaling Alters the Proteomic Profile of Th17 Cells. In an effort to complement the transcriptomics and qPCR observations with protein-level evidence, we applied in-depth quantitative proteomics analyses, using a method that employs highly orthogonal 2D ultrahigh-performance liquid chromatography in combination with nanospray ultrahigh-resolution tandem mass spectrometry. Interestingly, 6,488 proteins were quantitatively profiled across all samples (peptide level $q < 0.01$), of which 409 were differentially expressed in act-A–Th17 cells (Fig. 8*E*). Principal component analysis of differentially expressed proteins (DEPs) showed that act-A–Th17 cells clustered separately from control-treated Th17 cells (*SI Appendix*, Fig. S7*A*). Selected DEPs, along with the biological process they participate in, are depicted in a heatmap format (Fig. 8*E*). Notably, certain of the DEPs were also identified in the RNA-seq datasets (Fig. 8*E*). GO analysis of the DEPs showed significant enrichment for key immunological pathways, including positive regulation of cell migration, negative regulation of T cell receptor signaling, activation of MAPK activity, methylation, positive regulation of transcription, and protein phosphorylation (Fig. 8*E*). IPA canonical pathway analyses identified a broad spectrum of differentiated cytosolic, membrane-bound, and secreted proteins that collectively predicted the activation of STAT3 in Th17 cells differentiated in the presence of activin-A, supporting the aforementioned mechanistic findings on activin-A–induced STAT3 activation ($P = 4.0$ e-3; z-score = 2.0) (Fig. 8*F*). Moreover, IPA demonstrated a significant enrichment of the T cell receptor ($P = 5.2$ e-4) and the NF-κB signaling pathways among the DEPs in act-A–Th17 cells ($P = 1.3$e-3).

To decipher the clinical relevance of our in vivo findings, we isolated human naive $CD4^+$ T cells from RRMS patients (and healthy controls) and polarized them toward the Th17 cell lineage, in the presence or absence of activin-A. Similar to our observations in mouse T cells, activin-A stimulation decreased the expression of factors associated with pathogenic Th17 cells, such as, *Ifng*, *Tbx21*, and *Csf2*, while it enhanced *Cyp1a1* and *Nt5e* expression (Fig. 8*G* and *SI Appendix*, Fig. S7*A*). IFN-γ and IL-17 protein levels were significantly decreased, while IL-10 was up-regulated in human Th17 cells differentiated in the presence of activin-A (Fig. 8*H* and *SI Appendix*, Fig. S7*B*). Subsequently, we determined whether activin-A signaling can restrain robust inflammatory responses generated by $CD4^+$ T effector cells in RRMS patients and healthy donors. Indeed, treatment of anti-CD3/CD28-activated $CD4^+$ T effectors with activin-A decreased IFN-γ and IL-17 production, concomitant with increased IL-10 levels (*SI Appendix*, Fig. S7*C*). Finally, we analyzed the correlation between serum activin-A and IFN-γ, IL-17, and IL-10 levels in $CD4^+$ T effectors restimulated ex vivo. A negative correlation between serum activin-A levels and IFN-γ and IL-17 production in $CD4^+$ T cells from RRMS patients was observed, while a positive correlation was identified between higher IL-10 expression in $CD4^+$ T cells and activin-A release in the serum (*SI Appendix*, Fig. S7*D*). These findings suggest that activin-A signaling also restrains proinflammatory human Th17 cell responses generated in the context of RRMS.

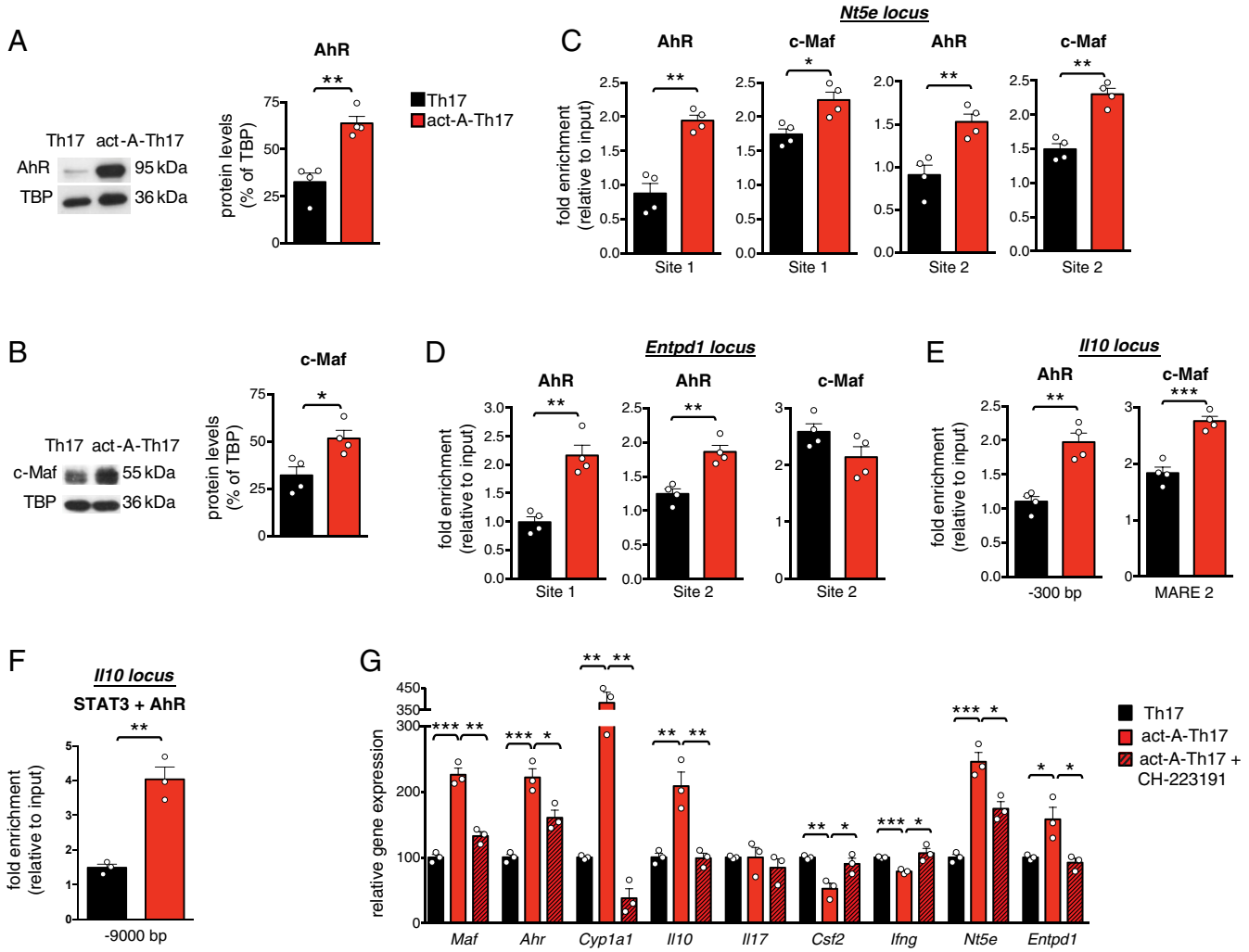

Fig. 7. AhR drives activin-A–mediated up-regulation of CD73 and antiinflammatory genes in Th17 cells. (*A*) Representative immunoblots showing AhR and c-Maf protein levels in act-A–Th17 or Th17 cells. (*B*) Quantification of relative AhR and c-Maf expression is shown; TATA binding protein (TBP). Data are mean ± SEM; each symbol corresponds to one of four independent in vitro experiments. (*C*) ChIP analyses demonstrating the binding of AhR and c-Maf on the *Nt5e* locus. Data are mean ± SEM; each symbol represents one of four independent in vitro experiments. (*D*) ChIP analyses demonstrating the binding of AhR and c-Maf on the *Entpd1* locus and (*E*) on the *Il10* locus. Data are mean ± SEM; each symbol represents one of four independent in vitro experiments. (*F*) Sequential ChIP analysis demonstrating STAT3 and AhR cobinding on the *Il10* conserved noncoding sequence-9 (−9.0 kb) locus. Data are mean ± SEM; each symbol corresponds to one of three independent in vitro experiments. (*G*) Act-A–Th17 or Th17 cells were differentiated, in the presence of the AhR antagonist, CH-223191 or control (DMSO). Gene expression was analyzed by qPCR and normalized to *Gapdh* and *Polr2a*. Each symbol represents the mean ± SEM of duplicate wells and corresponds to one of three independent in vitro experiments. Statistical analysis was performed by unpaired Student's *t* test; $*P < 0.05$, $**P < 0.01$ and $***P < 0.001$.

Discussion

Identification of the factors that control the balance between pathogenic and nonpathogenic Th17 cell states is essential for exploiting their beneficial host defense functions, while preventing their detrimental effects that trigger autoimmune diseases (2, 3). The present study demonstrates that systemic administration of activin-A ameliorates EAE severity, associated with decreased activation of Th17 cells. Notably, activin-A coopts a CD73-dependent molecular pathway that silences pathogenic gene expression and inhibits encephalitogenic functions of Th17 cells. Concomitantly, activin-A activates AhR, c-Maf, and STAT3 signaling to boost antiinflammatory gene programs in Th17 cells. Interestingly, activin-A–induced suppression of Th17 pathogenicity is associated with negative regulation of Hif1-α, pointing to a link between activin-A signaling and metabolic regulation in Th17 cells.

Activin-A exerts neuroprotective effects in animal models of stroke and excitotoxic injury (43, 44). Moreover, oligodendrocyte differentiation and myelination are impaired in mice with oligodendrocyte-specific deletion of ALK4, emphasizing potent CNS-repairing functions for activin-A (45). Activin-A is also up-regulated in microglia and macrophages with an M2-like phenotype, considered to exert tissue-repair functions (46). Still, the effects of activin-A on encephalitogenic T cell responses and associated CNS autoimmunity remain unexplored. Here, we discovered that administration of activin-A attenuated EAE and this was at least partly mediated by inhibition of Th17 effector responses. This was evidenced by decreased infiltration of pathogenic IL-17/IFN-γ double-positive $CD4^+$ T cells in the CNS, accompanied by impaired autoantigen-driven recall T cell responses in the DLNs. In addition, administration of activin-A restrained the infiltration of inflammatory myeloid cells in the CNS, concomitant with a reduction in GM-CSF, IL-1β, and TNF-α, cytokines that govern myeloid cell recruitment and EAE pathogenesis. Studies by our group and others have highlighted crucial roles of activin-A in Th cell differentiation and effector functions (19–23). The present

findings expand the array of functions of this pleiotropic cytokine uncovering a crucial role for activin-A in the suppression of Th17 responses and linked CNS autoimmunity.

An intriguing finding of our studies was that activin-A signaling through its canonical pathways inhibited the differentiation of Th17 cells with pathogenic properties, as evidenced by repression of a constellation of genes linked to Th17 pathogenicity, including *Ifng*, *Csf2*, *Il1b*, *Tbx21*, and *Batf* (9–11, 24, 25, 47). In addition, Th17 cells generated in the presence of activin-A exhibited decreased encephalitogenicity, as evidenced by diminished ability to elicit EAE upon transfer in vivo. Concomitantly, we discovered that activin-A/ALK4 signaling up-regulated the expression of antiinflammatory genes associated with nonpathogenic Th17 cells, such as *Il10*, *Maf*, and *Ahr* (9–11, 24, 25, 29, 47). Seeking to uncover the molecular mechanisms involved, we identified the CD73 ectonucleotidase as a critical driver of activin-A–induced suppression of the pathogenic signature and encephalitogenic functions of Th17 cells. Previous studies have demonstrated that CD73 expression in Th17 cells is dependent on IL-6–induced STAT3 activation and TGF-β–mediated inhibition of the transcriptional repressor, Gfi-1 (34). Here, we demonstrated that activin-A also engages STAT3-dependent pathways to up-regulate CD73 expression in Th17 cells; however, its effects were independent of Gfi-1 or TGF-β signaling. In agreement with our findings, CD73 is induced in TGF-β receptor-deficient $CD4^+$ T cells (48), suggesting that its expression is also regulated by other factors. Notably, we detected decreased STAT3 phosphorylation in Th17 cells upon inhibition of Smad2/3 signaling pathways. In a reciprocal manner, recent studies have demonstrated that activin-A up-regulates connective tissue growth factor (CTGF) expression in endometrial cells through STAT3-induced Smad2/3 phosphorylation (49). Altogether, these studies uncovering a link between Smad2/3 and STAT3 intracellular signaling pathways downstream of activin-A activation.

Interestingly, through analyses of ChIP-seq datasets we detected enriched binding of Th17 cell-associated TFs, including STAT3, c-Maf, and RORγt, along with the histone modifications H3K4me1 and H3K27me1, at a novel site (+1,700 bp) on the *Nt5e* gene, highlighting this region as a potentially important regulatory hub controlling CD73 expression. Indeed, we detected enriched binding of c-Maf to this site in act-A–Th17 cells, uncovering a previously unidentified role of c-Maf in regulating *Nt5e* transcription. We also found that c-Maf controlled IL-10 up-regulation in act-A–Th17 cells through enhanced binding to the *Il10* locus. Together with recent studies demonstrating impaired IL-10 expression in *Maf* $^{-/-}$ Th17 cells, these findings emphasize the central role of c-Maf in regulating IL-10 expression in Th17 cells (50). Apart from c-Maf, a striking increase in AhR levels was detected in Th17 cells differentiated with activin-A. We also discovered enriched binding of AhR on the *Nt5e*, *Entpd1*, and *Il10* loci in act-A–Th17 cells. Interestingly, our findings demonstrated that STAT3 forms a multipartite transcriptional complex with AhR and ARNT that seems to be important in activin-A–induced *Il10* up-regulation in Th17 cells. Inhibition of AhR signaling reversed activin-A–induced up-regulation of *Nt5e*, *Entpd1*, *Il10*, and *Maf* in Th17 cells, while it restored *Csf2* and *Ifng*. Considering that AhR drives the differentiation of distinct Th cell subsets, including $Foxp3^+$ Tregs, Th17, and Tr1 cells in response to divergent cytokines and environmental cues (8, 26, 29, 38, 39), our findings add activin-A to the increasing number of factors that integrate AhR signaling to shape Th responses.

Activin-A coopted CD39 and CD73 functions to reduce inflammatory eATP concentrations in Th17 cells. Moreover, activin-A decreased the protein levels of ATP-induced Hif1-α in Th17 cells through up-regulation of the Hif1-α inhibitors, Phd-1 and Phd-2 (29, 40, 41). In fact, we showed that negative regulation of Hif1-α was essential for activin-A–mediated suppression of the pathogenic Th17 profile. Altogether, these findings propose a mechanism wherein activin-A signaling through its canonical pSmad2/3 pathways induces AhR, STAT3, and c-Maf activation which drive CD39 and CD73 up-regulation in Th17 cells that, in turn, deplete eATP, dampen Hif1-α signaling, and restrain Th17 pathogenicity (*SI Appendix*, Fig. S8). Notably, our proteomics analyses highlighted the pleiotropic effects of activin-A on Th17 responses, as evidenced by perturbations in T cell receptor and NF-κB signaling pathways and activation of MAPK activity, phosphorylation, and histone methylation, molecular pathways that are closely linked to Th17 cell differentiation and pathogenicity (7, 34, 47).

Of translational relevance, we discovered increased activin-A levels in the serum and cerebrospinal fluid of RRMS patients. Considering the enhanced immunosuppressive effects of activin-A in EAE, increased activin-A expression in the context of MS may seem counterintuitive. Still, similar findings have been documented for IL-10 and TGF-β expression in RRMS patients, supporting the notion that although these immunoregulatory factors are increased, their functions and their signaling components may be compromised possibly as a result of the highly inflammatory tissue milieu (51–53). Moreover, limitations and confounding variables (i.e., medication) often observed when profiling biological fluids from small cohorts of individuals may also affect our findings and follow-up studies in larger cohorts should be conducted. Interestingly, activin-A stimulation restrained the differentiation of human Th17 cells with pathogenic properties. Concomitantly, activin-A decreased IFN-γ and IL-17 release and up-regulated IL-10 levels by T effector cells from RRMS patients and healthy controls. Overall, these findings support the notion that stimulation of CNS-reactive Th17 cells from RRMS patients with activin-A may bestow them with antiinflammatory, tissue-protective properties and follow-up studies will address this clinically important question.

In conclusion, our findings uncover functions of activin-A in suppressing mouse and human Th17 pathogenic responses and controlling CNS autoimmunity. Considering that ongoing clinical trials are targeting Th17 pathogenicity for the therapy of autoimmune diseases, our findings open up new opportunities for the exploitation of activin-A and its signaling pathways as therapeutic targets for the management of MS.

Materials and Methods

A detailed description of the materials and methods is provided in *SI Appendix*, *SI Materials and Methods*.

Human Subjects. Human participants signed an informed consent form and the study protocol was approved by the Scientific Research Ethics Committees of "G. Gennimatas" General State Hospital of Athens and the Athens Naval Hospital.

Induction of Active EAE and Scoring. EAE was induced as described previously (54). Recombinant activin-A (4 μg per mouse per dose; R&D Systems) or PBS were administrated (intraperitoneally) every 3 d, after EAE onset (days 10 to 12 or when reaching a clinical score >1), until killed. Dose–response experiments determined the optimal activin-A dose. Mice were killed at different time points during the course of the disease. At killing, cells were isolated from cervical and branchial DLNs and spinal cords for further experimentation. In recall assays, 5×10^4 DLN cells were cultured in 96-well U-bottom plates and stimulated with 20 μg/mL $MOG_{35–55}$ peptide. Cells were pulsed after 72 h of culture with ^{3}[H]-thymidine (1 μCi per well; Perkin-Elmer) and harvested 12 h later on a filter using a cell harvester (17, 18).

Mice. Animal handling and procedures were in accordance with a National Institutes of Health Statement of Compliance (Assurance) with Standards for Humane Care and Use of Laboratory Animals (#A5736-01 and A38 516 10006), in compliance with the Johns Hopkins Animal Care and Use Policies, and with the European Union Directive 86/609/EEC on protection of animals used for experimental purposes.

T Cell Transfer Model of EAE. C57BL/6 mice were immunized with CFA and $MOG_{35–55}$ peptide, as described previously (54). DLN cells were harvested on day 10 after immunization and restimulated ex vivo with 20 μg/mL

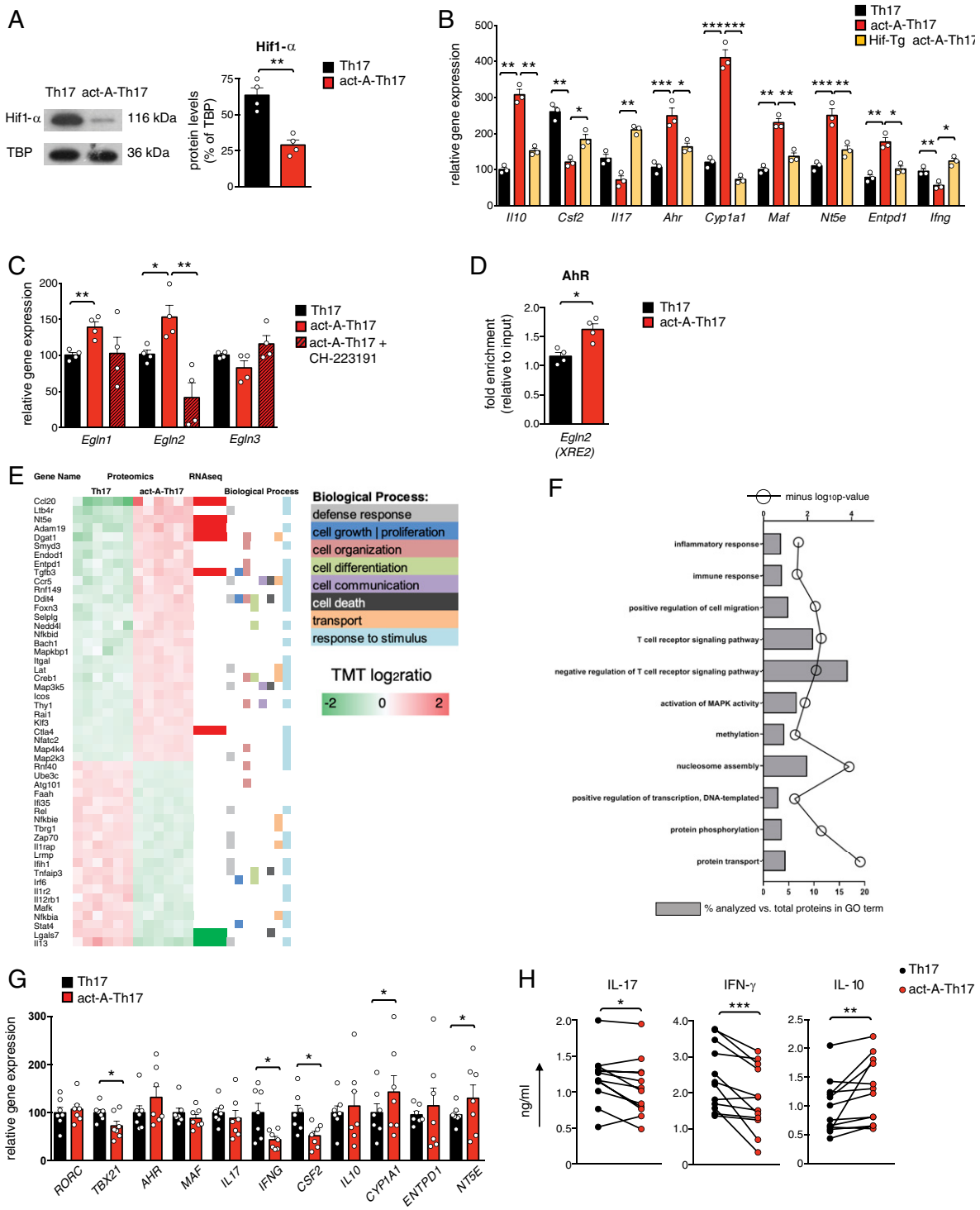

Fig. 8. Hif1-α suppression is crucial for activin-A–mediated modulation of the pathogenic Th17 cell signature. (*A*) Representative immunoblots showing Hif1-α expression. Quantification of relative Hif1-α protein levels are depicted; TATA binding protein (TBP). Data are mean ± SEM; each symbol corresponds to one of four independent in vitro experiments. (*B*) Gene expression of act-A–Th17 or Th17 cells from C57BL/6 or Hif1-Tg/CD4 mice was analyzed by qPCR and normalized to *Gapdh*. Each symbol represents the mean ± SEM of triplicate wells and corresponds to one of three independent in vitro experiments. (*C*) Act-A–Th17 or Th17 cells were differentiated in the presence of CH-223191 or DMSO. Gene expression was analyzed by qPCR and normalized to *Gapdh* and *Polr2a*. Each symbol is the mean ± SEM of duplicate wells and corresponds to one of four independent in vitro experiments. (*D*) ChIP analysis demonstrates the binding of AhR on the XRE2 site in the *Egln2* locus. Results are mean ± SEM; each symbol corresponds to one of four independent in vitro experiments. (*E*) Heatmap of DEPs in act-A–Th17 cells vs. Th17 cells, along with the biological processes they participate. The proteomics dataset was aligned with the RNA-seq dataset and a subset of the DEPs was verified to exhibit differential expression at the mRNA level. (*F*) GO analysis of DEPs in act-A–Th17 cells. (*G*) Naive $CD4^+$ T cells from RRMS patients were polarized toward the Th17 cell lineage, as indicated. Gene expression was analyzed by qPCR and normalized to *B2M*. Data are mean ± SEM of duplicate wells; each symbol depicts an individual donor ($n = 7$ donors). (*H*) Cytokine release in culture supernatants. Each symbol represents the mean ± SEM of triplicate wells and corresponds to an individual donor ($n = 12$ donors). Statistical analysis was performed by unpaired Student's *t* test and Wilcoxon matched-pairs signed rank test; $^*P < 0.05$, $^{**}P < 0.01$ and $^{***}P < 0.001$.

$MOG_{35–55}$ peptide, IL-23 (20 ng/mL; R&D Systems) (Th17 conditions) in the presence of PBS or activin-A (100 ng/mL), for 72 h. $CD4^+$ T cells were isolated and adoptively transferred (3×10^6 per mouse) intraperitoneally to C57BL/6-*Rag1*$^{-/-}$ naive recipients and 48 h later, pertussis toxin (PTX) was administered as above. Mice were monitored clinically at least until day 30. In another set of experiments, Th17 or act-A–Th17 cells (3×10^6), generated as above, were treated with anti-CD73 blocking antibody (BioXCell; 20 μg/mL) or IgG control, and then adoptively transferred to C57BL/6-*Rag1*$^{-/-}$ mice (day 0) as above. C57BL/6-*Rag1*$^{-/-}$ mice were administered (intraperitoneally) with anti-CD73 (50 μg per mouse) or IgG control on days 4, 7, 10, and 14 after T cell transfer. In other experiments, Th17 or act-A–Th17 cells (3×10^6) were generated as above from CFA/MOG-immunized *Nt5e*$^{-/-}$ or *Nt5e*$^{+/+}$ and transferred into C57BL/6-*Rag1*$^{-/-}$ mice (day 0).

In Vitro Mouse T Cell Differentiation. $CD4^+CD62L^+$ naive T cells were isolated by magnetic beads (Miltenyi Biotec) or sorted on a BD FACSAria II sorter from the spleens and lymph nodes of C57BL/6, Hif1-Tg/CD4 *I17a*^{Cre}/*R26R*^{eYFP} or *Egln2*$^{-/-}$ mice and activated with plate-bound anti-CD3 (eBioscience; 1 μg/mL) and soluble anti-CD28 (eBioscience; 1 μg/mL) in 96-well plates, for 3 to 4 d. For Th17 cell differentiation, 10^5 naive T cells were supplemented with recombinant IL-6 (Peprotech; 20 ng/mL), IL-1β (Peprotech; 20 ng/mL), and IL-23 (R&D Systems; 20 ng/mL) in the presence of PBS (control) or activin-A (100 ng/mL) (9). Dose–response experiments determined the optimal concentrations of anti-CD3/anti-CD28 antibodies and activin-A. In some experiments, the AhR antagonist (CH-223191, 5 μM; Sigma-Aldrich), the CD73 antagonist (AMP-CP, 100 μM; Sigma-Aldrich), the Smad3 inhibitor (SIS3, 20 μm; Sigma-Aldrich), the neutralizing anti-ALK4 antibody (10 μg/mL; R&D), the STAT3 inhibitor (STA-21, 10 μM; Cayman Chemical) or vector (PBS) were administered in T cell cultures, as indicated. Cells were harvested on days 3 to 4 postdifferentiation for RNA extraction and on days 3 to 9 for extracellular or intracellular flow-cytometry staining and cytokine analyses in culture supernatants.

ACKNOWLEDGMENTS. We thank A. Apostolidou for assistance with flow cytometry and sorting; A. Agapaki and S. Psarras for histology preparations; and Eleni Rigana and Stamatis Pagakis for assistance with the confocal microscopy imaging.

1. C. A. Dendrou, L. Fugger, M. A. Friese, Immunopathology of multiple sclerosis. *Nat. Rev. Immunol.* **15**, 545–558 (2015).
2. T. Korn, A. Kallies, T cell responses in the central nervous system. *Nat. Rev. Immunol.* **17**, 179–194 (2017).
3. P. R. Burkett, G. Meyer zu Horste, V. K. Kuchroo, Pouring fuel on the fire: Th17 cells, the environment, and autoimmunity. *J. Clin. Invest.* **125**, 2211–2219 (2015).
4. G. R. Dos Passos, D. K. Sato, J. Becker, K. Fujihara, Th17 cells pathways in multiple sclerosis and neuromyelitis optica spectrum disorders: Pathophysiological and therapeutic implications. *Mediators Inflamm.* **2016**, 5314541 (2016).
5. D. Matusevicius *et al*., Interleukin-17 mRNA expression in blood and CSF mononuclear cells is augmented in multiple sclerosis. *Mult. Scler.* **5**, 101–104 (1999).
6. J. S. Tzartos *et al*., Interleukin-17 production in central nervous system-infiltrating T cells and glial cells is associated with active disease in multiple sclerosis. *Am. J. Pathol.* **172**, 146–155 (2008).
7. B. Stockinger, S. Omenetti, The dichotomous nature of T helper 17 cells. *Nat. Rev. Immunol.* **17**, 535–544 (2017).
8. Y. Lee *et al*., Induction and molecular signature of pathogenic TH17 cells. *Nat. Immunol.* **13**, 991–999 (2012).
9. K. Ichiyama *et al*., The MicroRNA-183-96-182 cluster promotes T helper 17 cell pathogenicity by negatively regulating transcription factor Foxo1 expression. *Immunity* **44**, 1284–1298 (2016).
10. C. Wang *et al*., CD5L/AIM regulates lipid biosynthesis and restrains Th17 cell pathogenicity. *Cell* **163**, 1413–1427 (2015).
11. C. E. Zielinski *et al*., Pathogen-induced human TH17 cells produce IFN-γ or IL-10 and are regulated by IL-1β. *Nature* **484**, 514–518 (2012).
12. D. Hu *et al*., Transcriptional signature of human pro-inflammatory T_H17 cells identifies reduced IL10 gene expression in multiple sclerosis. *Nat. Commun.* **8**, 1600 (2017).
13. N. Gagliani *et al*., Th17 cells transdifferentiate into regulatory T cells during resolution of inflammation. *Nature* **523**, 221–225 (2015).
14. C. Heinemann *et al*., IL-27 and IL-12 oppose pro-inflammatory IL-23 in CD4+ T cells by inducing Blimp1. *Nat. Commun.* **5**, 3770 (2014).
15. M. P. Hedger, D. M. de Kretser, The activins and their binding protein, follistatin-Diagnostic and therapeutic targets in inflammatory disease and fibrosis. *Cytokine Growth Factor Rev.* **24**, 285–295 (2013).
16. W. Chen, P. Ten Dijke, Immunoregulation by members of the TGFβ superfamily. *Nat. Rev. Immunol.* **16**, 723–740 (2016).
17. C. P. Jones *et al*., Activin A and TGF-β promote T(H)9 cell-mediated pulmonary allergic pathology. *J. Allergy Clin. Immunol.* **129**, 1000–10.e3 (2012).
18. I. Morianos, G. Papadopoulou, M. Semitekolou, G. Xanthou, Activin-A in the regulation of immunity in health and disease. *J. Autoimmun.* **104**, 102314 (2019).
19. S. Huber *et al*., Activin a promotes the TGF-β-induced conversion of CD4+CD25- T cells into Foxp3+ induced regulatory T cells. *J. Immunol.* **182**, 4633–4640 (2009).
20. M. Locci *et al*., Activin A programs the differentiation of human TFH cells. *Nat. Immunol.* **17**, 976–984 (2016).
21. M. Semitekolou *et al*., Activin-A induces regulatory T cells that suppress T helper cell immune responses and protect from allergic airway disease. *J. Exp. Med.* **206**, 1769–1785 (2009).
22. S. Tousa *et al*., Activin-A co-opts IRF4 and AhR signaling to induce human regulatory T cells that restrain asthmatic responses. *Proc. Natl. Acad. Sci. U.S.A.* **114**, E2891–E2900 (2017).
23. L. Berod *et al*., De novo fatty acid synthesis controls the fate between regulatory T and T helper 17 cells. *Nat. Med.* **20**, 1327–1333 (2014).
24. P. W. F. Karmaus *et al*., Metabolic heterogeneity underlies reciprocal fates of T_H17 cell stemness and plasticity. *Nature* **565**, 101–105 (2019).
25. F. J. Quintana *et al*., Control of T(reg) and T(H)17 cell differentiation by the aryl hydrocarbon receptor. *Nature* **453**, 65–71 (2008).
26. K. Hirota *et al*., Fate mapping of IL-17-producing T cells in inflammatory responses. *Nat. Immunol.* **12**, 255–263 (2011).
27. A. L. Croxford, F. C. Kurschus, A. Waisman, Cutting edge: An IL-17F-CreEYFP reporter mouse allows fate mapping of Th17 cells. *J. Immunol.* **182**, 1237–1241 (2009).
28. I. D. Mascanfroni *et al*., Metabolic control of type 1 regulatory T cell differentiation by AHR and HIF1-α. *Nat. Med.* **21**, 638–646 (2015).
29. S. Deaglio *et al*., Adenosine generation catalyzed by CD39 and CD73 expressed on regulatory T cells mediates immune suppression. *J. Exp. Med.* **204**, 1257–1265 (2007).
30. J. H. Mills *et al*., CD73 is required for efficient entry of lymphocytes into the central nervous system during experimental autoimmune encephalomyelitis. *Proc. Natl. Acad. Sci. U.S.A.* **105**, 9325–9330 (2008).
31. G. Hernandez-Mir, M. J. McGeachy, CD73 is expressed by inflammatory Th17 cells in experimental autoimmune encephalomyelitis but does not limit differentiation or pathogenesis. *PLoS One* **12**, e0173655 (2017).
32. M. Jakovljevic *et al*., Down-regulation of NTPDase2 and ADP-sensitive P2 purinoceptors correlate with severity of symptoms during experimental autoimmune encephalomyelitis. *Front. Cell. Neurosci.* **11**, 333 (2017).
33. F. Chalmin *et al*., Stat3 and Gfi-1 transcription factors control Th17 cell immunosuppressive activity via the regulation of ectonucleotidase expression. *Immunity* **36**, 362–373 (2012).
34. M. Ciofani *et al*., A validated regulatory network for Th17 cell specification. *Cell* **151**, 289–303 (2012).
35. Y. Jiang *et al*., Epigenetic activation during T helper 17 cell differentiation is mediated by Tripartite motif containing 28. *Nat. Commun.* **9**, 1424 (2018).
36. X.-P. Yang *et al*., Opposing regulation of the locus encoding IL-17 through direct, reciprocal actions of STAT3 and STAT5. *Nat. Immunol.* **12**, 247–254 (2011).
37. L. Apetoh *et al*., The aryl hydrocarbon receptor interacts with c-Maf to promote the differentiation of type 1 regulatory T cells induced by IL-27. *Nat. Immunol.* **11**, 854–861 (2010).
38. R. Gandhi *et al*., Activation of the aryl hydrocarbon receptor induces human type 1 regulatory T cell-like and Foxp3(+) regulatory T cells. *Nat. Immunol.* **11**, 846–853 (2010).
39. L. Z. Shi *et al*., HIF1α-dependent glycolytic pathway orchestrates a metabolic checkpoint for the differentiation of TH17 and Treg cells. *J. Exp. Med.* **208**, 1367–1376 (2011).
40. E. V. Dang *et al*., Control of T(H)17/T(reg) balance by hypoxia-inducible factor 1. *Cell* **146**, 772–784 (2011).
41. P. C. Mahon, K. Hirota, G. L. Semenza, FIH-1: A novel protein that interacts with HIF-1alpha and VHL to mediate repression of HIF-1 transcriptional activity. *Genes Dev.* **15**, 2675–2686 (2001).
42. S. E. Weinberg *et al*., Mitochondrial complex III is essential for suppressive function of regulatory T cells. *Nature* **565**, 495–499 (2019).
43. B. Buchthal, U. Weiss, H. Bading, Post-injury nose-to-brain delivery of activin A and SerpinB2 reduces brain damage in a mouse stroke model. *Mol. Ther.* **26**, 2357–2365 (2018).
44. D. Lau, C. P. Bengtson, B. Buchthal, H. Bading, BDNF reduces toxic extrasynaptic NMDA receptor signaling via synaptic NMDA receptors and nuclear-calcium-induced transcription of inhba/activin A. *Cell Rep.* **12**, 1353–1366 (2015).
45. A. Dillenburg *et al*., Activin receptors regulate the oligodendrocyte lineage in health and disease. *Acta Neuropathol.* **135**, 887–906 (2018).
46. V. E. Miron *et al*., M2 microglia and macrophages drive oligodendrocyte differentiation during CNS remyelination. *Nat. Neurosci.* **16**, 1211–1218 (2013).
47. J. T. Gaublomme *et al*., Single-cell genomics unveils critical regulators of Th17 cell pathogenicity. *Cell* **163**, 1400–1412 (2015).
48. F. S. Regateiro *et al*., Generation of anti-inflammatory adenosine by leukocytes is regulated by TGF-β. *Eur. J. Immunol.* **41**, 2955–2965 (2011).
49. Z. Zhang *et al*., Activin a promotes myofibroblast differentiation of endometrial mesenchymal stem cells via STAT3-dependent Smad/CTGF pathway. *Cell Commun. Signal.* **17**, 45 (2019).
50. L. Gabryšová *et al*., c-Maf controls immune responses by regulating disease-specific gene networks and repressing IL-2 in $CD4^+$ T cells. *Nat. Immunol.* **19**, 497–507 (2018).
51. A. L. Ji, Z. H. Liu, W. W. Chen, W. J. Huang, The clinical significance of level changes of hs-CRP, IL-10 and TNF for patients with MS during active and relieving period. *Eur. Rev. Med. Pharmacol. Sci.* **20**, 4274–4276 (2016).
52. J. Mellergård, M. Edström, M. Vrethem, J. Ernerudh, C. Dahle, Natalizumab treatment in multiple sclerosis: Marked decline of chemokines and cytokines in cerebrospinal fluid. *Mult. Scler.* **16**, 208–217 (2010).
53. J. D. Lünemann, O. Aktas, P. Gniadek, R. Zschenderlein, F. Zipp, Downregulation of transforming growth factor-beta1 in interferon-beta1a-treated MS patients. *Neurology* **57**, 1132–1134 (2001).
54. I. M. Stromnes, J. M. Goverman, Active induction of experimental allergic encephalomyelitis. *Nat. Protoc.* **1**, 1810–1819 (2006).